Visual Abstract

# Investigation of the effect of impact load on concrete-filled steel tube columns under fire

Ali Golsoorat Pahlaviani
*Central Tehran Branch, Islamic Azad University, Tehran, Iran.*
*Ali.golsoorat_pahlaviani@iauctb.ac.ir*

Ali Mohammad Rousta
*Department of Civil Engineering, Yasouj University, Yasouj, Iran.*
*arousta@yu.ac.ir*

Peyman Beiranvand
*Department of Civil Engineering, Razi University, Kermanshah, Iran.*
*Peyman51471366@gmail.com, http://orcid.org/0000-0001-9384-8542*

**ABSTRACT.** Concrete-filled steel tube (CFST) columns are increasingly used in the construction of high-rise buildings which require high strength and large working space especially at lower stories. As compared to reinforced concrete columns, existence of the exterior steel tube not only bears a portion of axial load but also most importantly provides confinement to the infill concrete.with the confinement provided by the steel tube, axial strength of the infill concrete can be largely enhanced.this paper presents the investigation effect of impact load on concrete-filled steel tube columns under fire by numerical simulations using ABAQUS software.the results indicate that the CFST sections with larger confinement factor ξ=1.23 behaved in a very ductile manner under lateral impact. And the sections with smaller confinement factor ξ=0.44 generally behaved in a brittle mechanism.

**KEYWORDS.** Concrete-Filled Steel Tube; Impact load; Confinement factor.

OPEN ACCESS

**Citation:** Golsoorat Pahlaviani, A., Rousta, A.M., Beiranvand, P., Investigation of the effect of impact load on concrete-filled steel tube columns under fire, Frattura ed Integrità Strutturale, 54 (2020) 317-324.

**Received:** 20.04.2020
**Accepted:** 18.09.2020
**Published:** 01.10.2020



## INTRODUCTION

For concrete-filled steel tubes, Prichard and Perry conducted the drop-weight experiment to study the impact response of the confined concrete-filled steel tubes [1]. Chen et al. took into account the speed of impulsive loadings on concrete-filled steel tubes [2]. Li et al. carried out an experimental investigation and demonstrated impact resistance of concrete-filled steel tubes under axial dynamic loading [3]. Xiao et al. studied the impact responses of concrete-filled steel tubes and a high-speed gas gun was used in their research [4]. Huo et al. and Ren et al. used a Hopkinson pressure bar to study the axial impact resistance of microconcrete-filled steel tubes at elevated temperature [5,6]. Prion and Boehme have

investigated a number of concrete-filled steel column sections such that the two ends of sections were joints and there was loading on those two points. The results indicated that by increasing loading, loading capacity decreased severely before reaching to ultimate bending strength [7]. Marson and Bruneau conducted some experiments to survey the connection of foundation to concrete-filled steel column under the effect of impact load with diameter proportion of 34-64 thickness. The results suggest that with regard to cyclic curves, these types of sections have high ductility [8]. Also, Huo and et al. have performed experiments to examine the strength of concrete-filled steel sections under the effect of impact load with temperature increase up to 400°C. that in this paper, the validity of finite elements' results are carried out by using the results of tests done by Huo and et al. In present article, it is tried to investigate the behavior of concrete-filled steel columns under the effects of both impact loads and burning of it. Moreover, the effects of concrete confinement and interactions between steel section and concrete core will be considered [9]. Hao et al. studied the mechanical behavior of RPC filled square steel tube columns subjected to eccentric compression. The results show that, the failure form of the eccentrically loaded RPC filled square steel tubular column shows local buckling failure. Before the ultimate load is reached, there is no significant change on the surface of the specimen, and the yield stage of the load displacement curve is not obvious, either [10]. Jing et al. studied on the bond behavior of preplaced aggregate concrete-filled steel tube columns. In the study of Jing et al., parameters include the concrete strength, cross-section dimension and the thickness of steel tube were considered [11].Jing et al. studied on dynamic response of concrete-filled steel tube columns confined with FRP under blast loading. the results indicate that the constraints of FRP effectively enhance the blast resistance of the column, and the vulnerable parts mainly occur at the middle and two ends of the column. the blast resistance of the column can be enhanced by increasing the number of FRP layers or concrete strength. these results could provide a certain basis for blast resistance design of concrete-filled steel tubes confined with FRP [12].

## PROPERTIES OF MATERIALS

Mechanical and thermal features of steel and concrete are totally different. In this research, strength and stiffness of both materials will decrease. Stress-Strain curves of steel and concrete for room temperature (20°C) has been shown as T20 in Figs. 1 and 2. For all sections, the yield stress ($f_y$) has been considered as 350 N/mm², elasticity modulus ($E_s$) as 210000 N/mm² and compressive strength ($f_c$) as 30 N/mm² and strain ($\varepsilon_c$) as 0.0025. Stress-strain curve of steel under heat increase has been drawn on the basis of BS EN1993-1-2 [13] code and for concrete, it has been drawn based on BS EN1994-1-2 [14].

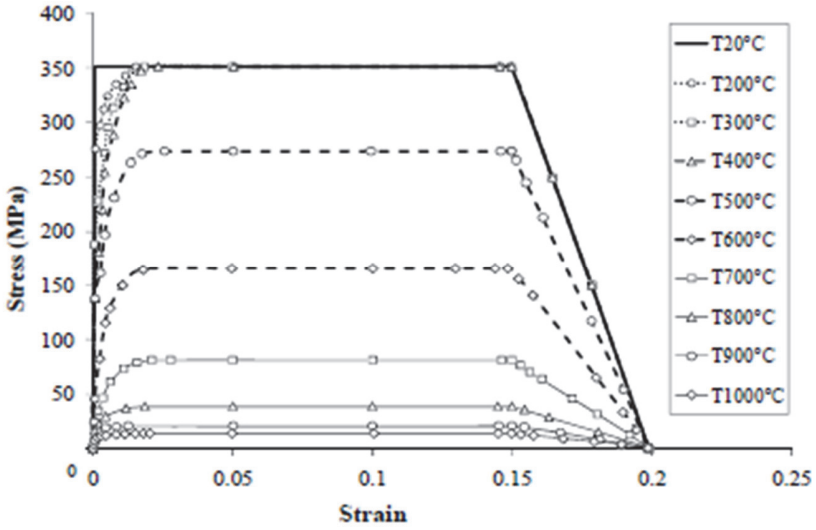


Figure 1: Stress-strain curve of steel under heat increase [13].

To simulate by Abaqus software, steel will be modeled according to real stress-strain relation which is obtained by Eqns. (1) and (2).

$$\sigma_{true} = \sigma_{nom}\left(1+\varepsilon_{nom}\right) \quad (1)$$

$$\varepsilon_{true} = ln\left(1+\varepsilon_{nom}\right) \tag{2}$$

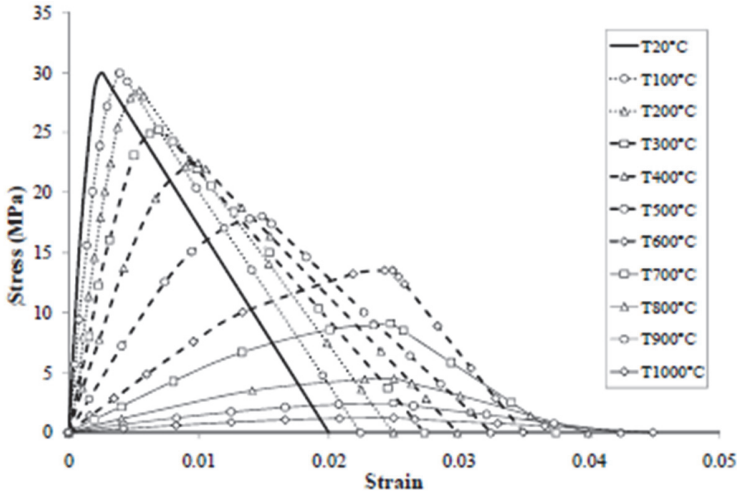


Figure 2: Stress-strain curve of concrete under heat increase [14].

In which $\varepsilon_{nom}$ and $\sigma_{nom}$ are nominal strain of section and nominal stress of section, respectively. The real value of steel stress and strain has been given in Tab. 1.

| Real Stress (MPa) | Plastic Strain |
|---|---|
| 300 | 0.000 |
| 350 | 0.025 |
| 375 | 0.100 |
| 394 | 0.200 |
| 400 | 0.350 |

Table 1: Real stress and strain values of steel.

To modeling concrete in plastic region and investigation of destruction in it, concrete plastic damage model has been used. The values of stress, strain, and plastic destruction of concrete are represented in Tab. 2 and 3.

| Tensile strength (MPa) | Fraction strain | Destruction parameter in tension |
|---|---|---|
| 35 | 000000.0 | 00.0 |
| 31.5 | 000176.0 | 25.0 |
| 58.0 | 001539.0 | 99.0 |

Table 2: Values of stress, strain and plastic destruction of concrete in tension.

| Tensile strength (MPa) | Fraction strain | Destruction parameter in compression |
|---|---|---|
| 17.5 | 0.000000 | 0.000 |
| 25.7 | 0.00038 | 0.112 |
| 34.9 | 0.00189 | 0.429 |
| 35 | 0.00218 | 0.466 |
| 38 | 0.00456 | 0.701 |

Table 3: Values of stress, strain and plastic destruction of concrete in compression.

Yield criterion Von Mises and isotropic hardening law have been used for modeling behavior of steel.in this model, the problems relevant to geometric nonlinear analysis were considered too and great transformation method has been used and due to contact elements between steel and concrete and appropriation of contact surface friction, asymmetric Newton-Raphson method has been implemented. Concrete core is defined by an eight-node hexahedral element or three transferred

degree of freedom in each node through C3D8R model. As it is seen in Fig. 3, concrete confinement has numerous effects on stress-strain diagram, therefore, the effect of concrete confinement has been considered in this model.

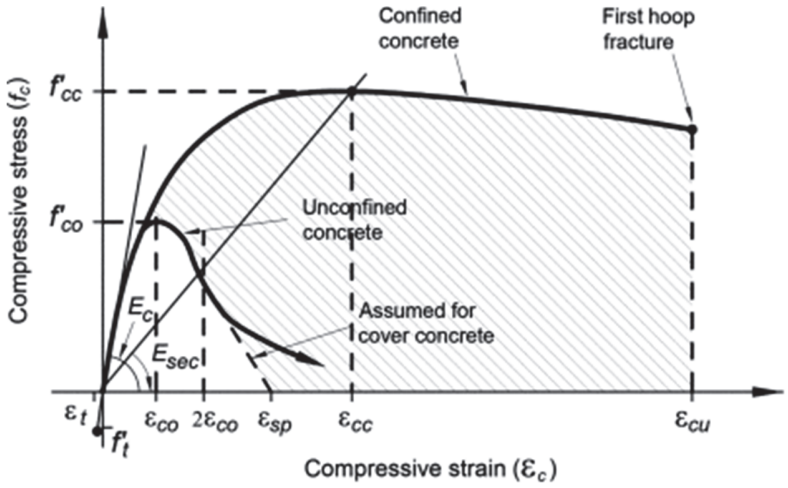


Figure 3: Effect of confinement on concrete stress-strain diagram [10]-

The steel wall has been defined by C3D8I element which as well as C3D8R element is described with eight nodes and three degree of freedom in each node and has suitable match with other elements used in the model. This element is able to transfer the compression in the direction of normal run and shear in the direction of tangent to surface. Steel tube and concrete are all solid elements and they are assimilated to shell elements.

## Description of Working Sections

The used sections in this research will be divided into two groups in the Tab. 4.
The values of impact loading ratio $\eta$ and value of confinement factor $\xi$ will be calculated according to Eqns. (3) and (4).

$$\eta = \frac{N_0}{N_u} \tag{3}$$

$$\xi = \frac{A_s f_y}{A_c f_c} \tag{4}$$

| Group | Sections | Dimensions of specimens (mm) | $\xi$ | Impact Velocity (m/s) | $\eta$ |
|---|---|---|---|---|---|
| 1 | CFST1 | 114×1.7 | 0.44 | 4.4 | 0.3 |
| | CFST2 | | | 4.4 | 0.6 |
| | CFST3 | | | 4.8 | 0.3 |
| 2 | CFST4 | 114×3.5 | 1.23 | 4.4 | 0.3 |
| | CFST5 | | | 11.7 | 0.3 |
| | CFST6 | | | 11.7 | 0.6 |

Table 4: The used sections in this research.

In these equations, $N_o$ is the value of applying load, $N_u$ is the loading capacity of section, $A_s$ is the steel cross sectional area and $A_c$ the concrete cross sectional area, $f_y$ is yield stress of steel and $f_c$ is the compressive strength of concrete. In this research, columns have been assumed as circular concrete-filled steel sections with ending conditions of two cantilevers and length of 1.2 meter.

## Numerical Simulations by Abaqus software

Concrete-filled steel tube structures can be modeled in Abaqus software in Fig. 4.
Then, by applying impact loads in the middle of the column, we investigated the impact load value according to loading time for sections Figs. 5 to 10.

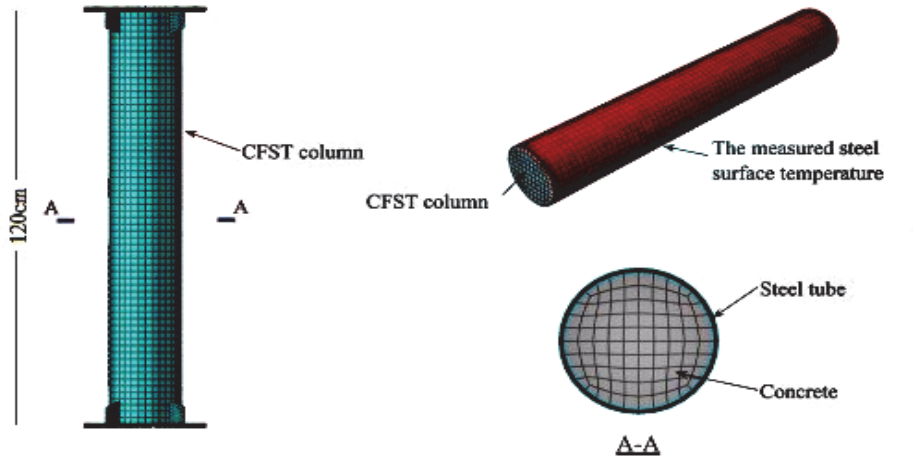


Figure 4: The finite element model of concrete-filled steel tube column.

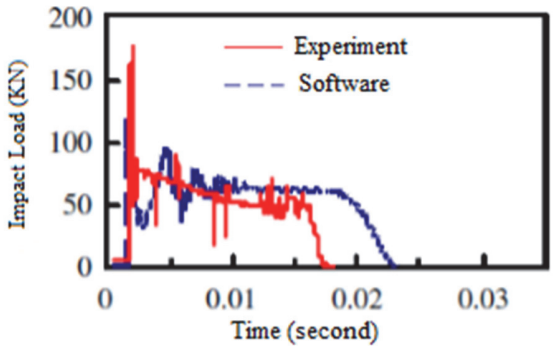


Figure 5: The impact load of CFST1 column according to loading time.

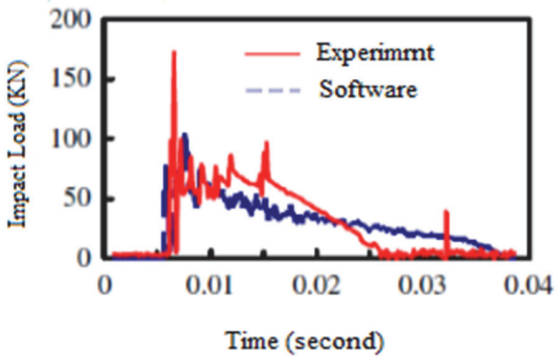


Figure 6: The impact load of CFST2 column according to loading time.

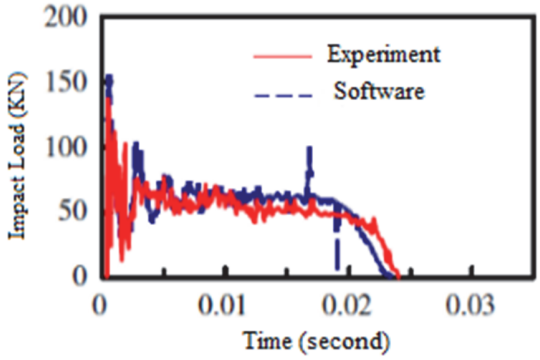


Figure 7: The impact load of CFST3 column according to loading time.

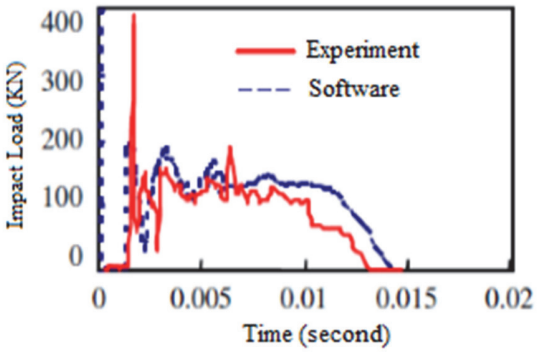


Figure 8: The impact load of CFST4 column according to loading time.

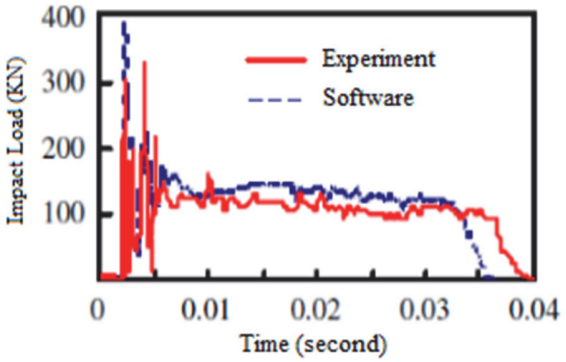


Figure 9: The impact load of CFST5 column according to loading time.

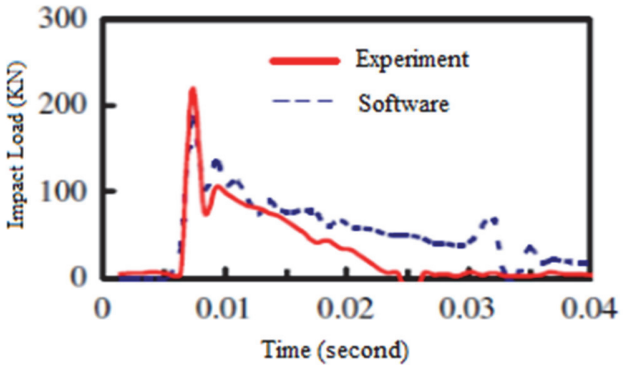


Figure 10: The impact load of CFST6 column according to loading time.

As it is observed, by increasing the thickness of steel section and confinement effect, section loading capacity resulted from impact load has been increased and also, the loading capacity of columns decreases in both groups by increasing $\eta$ value.in Figs. 11 and 12, the failure case of columns in group 1 and 2 under impact load are investigated.

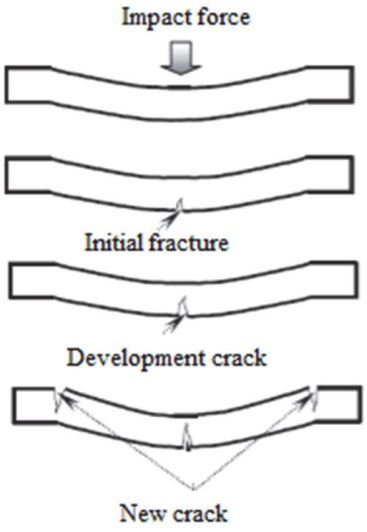


Figure 11: The whole trend of failure in columns of group 1 under the effect of impact loads.

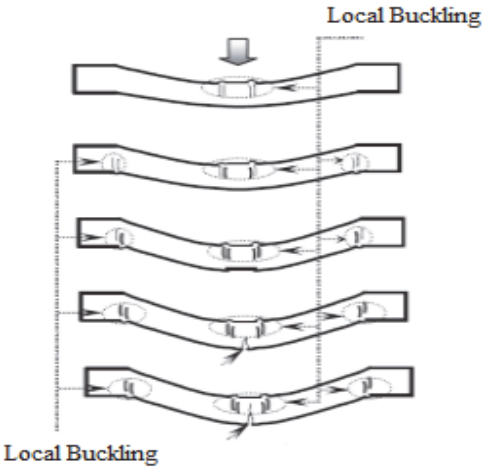


Figure 12: The whole trend of failure in columns of group 2 under the effect of impact loads.

As it is observed, increase of steel section thickness and confinement effect will lead to the postponement of initial failure and failure occurs only in the centre of the column span. In order to validate the finite element model with experimental results, we will examine the overall case of column failure under the effect of impact load in Figs. 13 and 14.
As it is observed, the results of failure in finite element model have high accordance with experimental results. In addition, we investigate the compressive stress shaped in concrete core under the effect of impact load as in Fig. 15.
As it is observed, a part of concrete core which is approximate to applied impact load is under the all-round pressure. Also, due to concrete core, the local buckling value of steel section has been limited basically and the ductility of concrete core will increase through the effect of confinement of steel section. Impact loading will be divided into sections A, B, C.
Case A: initiation of loading to maximum load value.
Case B: loading reduction and its permanency.
Case C: end of loading
Now in Figs. 16, 17, 18 plastic strain in steel section under the effect of impact load will be investigated in cases A, B, C.

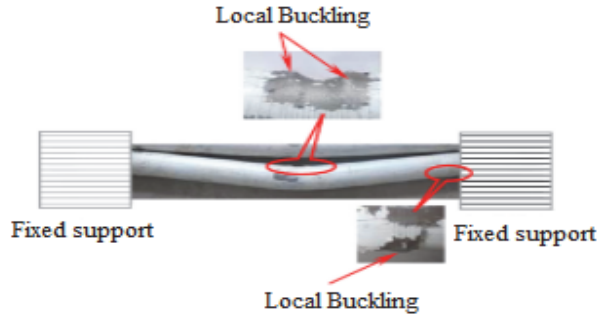


Figure 13: The overall schematic of failure in experimental model.

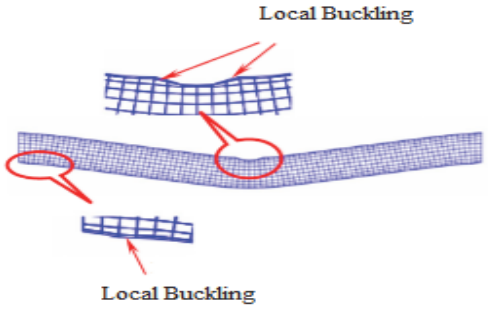


Figure 14: The overall schematic of failure in finite element model.

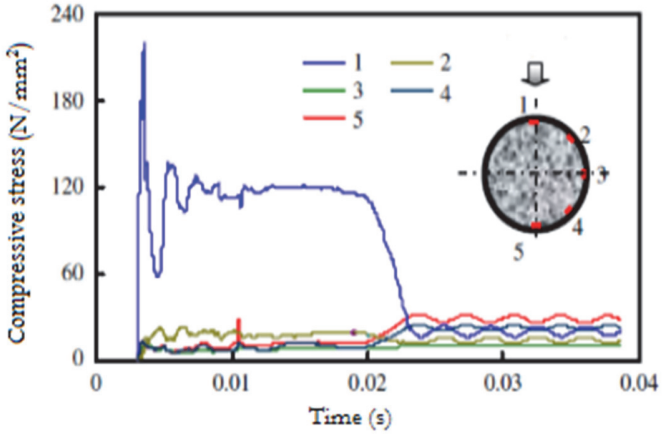


Figure 15: The overall schematic of failure in finite element model.


Figure 16: Plastic strain in steel section in case A.

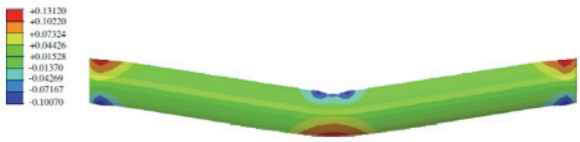

Figure 17: Plastic strain in steel section in case B

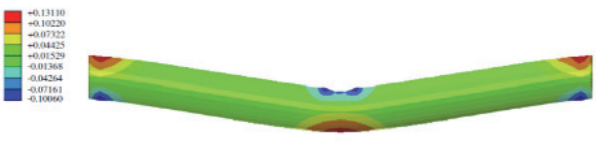

Figure 18: Plastic strain in steel section in case C

As it is observed, plastic transportation happens only in case A and plastic strain is also less than other cases. In case B, we have plastic transformation only in the centre of span and in case C, the distribution of plastic strain does not change very much in proportion to previous case or in other words, all other components of section in case C will have elastic transformation during reduction of impact load till end of loading.

## CONCLUSIONS

Increase in the thickness of steel section and confinement effect leads to increase the value of section loading capacity resulted from impact load.
By increasing the value of $\eta$, the loading capacity of columns decreases in any case.
By increasing the thickness of steel section and confinement effect in columns, the initial failure is postponed and failure takes place only in the center of column span. Of course, increasing the dimensions and thickness of steel section must be conditioned to meeting local buckling situations of codes.
The greater the dimensions of concrete-filled steel sections are, the temperature of concrete core decreases more and the time of resistance against fire will increase.
In section C, all components will have elastic transformation during the decrease of impact load up to end of loading and plastic transformation occurs only at the time of maximum impact loading.

## REFERENCES

[1] Prichard, S.J., Perry, S.H. (2000). The impact behavior of sleeved concrete cylinders, Structural Engineer, 78(17), pp. 23–27.
[2] Chen, Z.Y., Luo, J.Q., and Pan, X.W. (1986). Tsinghua University technical reports TR 4 of Research Laboratory of Earthquake and Blast Resistant Engineering: behaviour of reinforced concrete structural members subjected to impulsive loads 1986. Tsinghua University Press, Beijing (in Chinese).
[3] Li, Z., et al. (2006). The research of the dynamic property of steel tube confined concrete short column under axial impact loads, Journal of Taiyuan University of Technology, 37(4), pp. 383–385.
[4] Xiao, Y., et al. (2005). Impact tests of concrete-filled tubes and confined concrete filled tubes, Proc., 6th Int. Conf. on Shock and Impact Loads on Structures, School of Civil and Resource Engineering, Univ. of Western Australia, Perth, WA, Australia.
[5] Huo, J.S., Ren, X.H., and Xiao, Y. (2012). Impact behavior of concrete filled steel tubular stub columns under ISO-834 standard fire, China Civil Engineering Journal, 4(45), pp. 9–20.
[6] Ren, X.H., Huo, J.S., and Chen, B.S. (2011). Dynamic behaviors of concrete-filled steel tubular stub columns after exposure to high temperature, Journal of Vibration and Shock, 30(11), pp. 67–73.
[7] Prion, H.G.L., Boehme, J. (1994). Beam-Column Behaviour of Steel Tubes Filled with High Strength Concrete, Canadian Journal of Civil Engineering, 21, pp. 207-218.
[8] Marson, J. Bruneau, M. (2004). Cyclic Testing of Concrete-Filled Circular Steel Bridge Piers Having Encased Fixed-Base Detail, ASCE Journal of Bridge Engineering, 9(1), pp. 14-23.
[9] Huo, J.S., Zheng, Q., Chen, B.S., Xiao, Y. (2009). Tests on impact behaviour of micro-concrete-filled steel tubes at elevated temperatures up to 400 °C, Materials and Structures, 42(10), pp. 1325-1334.
[10] Hao, W., Xu, X., Niu, Z., N., (2018). Experimental study on the mechanical behavior of RPC filled square steel tube columns subjected to eccentric compression, Frattura ed Integrità Strutturale, 12(46), pp. 391-399.
[11] Jing, LV., Tianhua, Z., Qiang, D., Kunlun, L., Liangwei, J., (2020). Research on the Bond Behavior of Preplaced Aggregate Concrete-Filled Steel Tube Columns, Materials, 13(2), pp. 1-15.
[12] Jing, D., Junhai, Z., Dongfang, Z., Yingping, Li., (2019). Research on Dynamic Response of Concrete-Filled Steel Tube Columns Confined with FRP under Blast Loading, Shock and Vibration, pp. 1-18.
[13] BS EN 1993-1-2, (2005). Eurocode 3: Design of steel structures, Part 1.2: General rules structural fire design, London: British Standards Institution.
[14] BS EN 1994-1-2, (2005). Eurocode 4: Design of composite steel and concrete structures, Part 1.2: General rules-Structural fire design, London: British Standards Institution.